A Non-Orthogonal Multiple Access Assisted Integrated Sensing and Communication Network using Orthogonal Delay-Doppler Division Multiplexing

Salma Sultana*, Shuhao Zeng§, Ahmed Abdelhadi**, Husheng Li††, Zhu Han*, and H.Vincent Poor§,
*University of Houston, Houston, Texas, USA,
§Princeton University, Princeton, New Jersey, USA,
**University of North Dakota, Grand Forks, North Dakota, USA,
††Purdue University, West Lafayette, IN, USA,

***Abstract*—This work explores the integration of Non-Orthogonal Multiple Access (NOMA) and Orthogonal Delay-Doppler Division Multiplexing (ODDM) in an Integrated Sensing and Communication (ISAC) framework. The proposed system model leverages ODDM for high-mobility scenarios and NOMA for efficient resource utilization, thereby enabling enhanced communication and sensing trade-offs. To achieve a trade-off between communication and sensing performances, an optimization problem is formulated to maximize the weighted sum of sensing performance metric and communication throughput by jointly optimizing user grouping, power allocation, and beamforming, which, however, are coupled. To efficiently solve this problem, we decompose it into three subproblems, i.e., user grouping subproblem, power allocation subproblem, and beamforming subproblem, which are then solved in an iterative manner to improve system performances. Simulation results validate the efficacy of the framework under diverse mobility conditions, demonstrating improved sum-rate and sensing accuracy compared to Orthogonal Multiple Access (OMA) systems. This study provides insights into advanced ISAC architectures, critical for future 6G networks.**

***Index Terms*—ISAC, ODDM, NOMA.**

I. Introduction

The rapid advancements in wireless communication are driving the development of next-generation networks, such as 6G, which aim to meet the increasing demands for ultra-reliable and low-latency communication, massive connectivity, and integrated functionalities. One of the key paradigms in this evolution is the integration of Integrated Sensing and Communication (ISAC) [1], a framework that combines communication and environmental sensing within a unified system. ISAC offers the potential to enhance resource utilization and enable new services like vehicular networks, augmented reality, and autonomous systems, where communication and sensing are interdependent. By integrating these functions, ISAC [2] is poised to play a critical role in 6G networks, supporting applications in dynamic environments and high-mobility scenarios.

Non-Orthogonal Multiple Access (NOMA) is a critical enabler for ISAC systems in next-generation networks, allowing sensing and communication functionalities to share resources efficiently. By employing superposition coding and successive interference cancellation (SIC), NOMA enables simultaneous transmissions, significantly improving spectral efficiency compared to orthogonal approaches. In downlink ISAC, NOMA mitigates inter-user and sensing-to-communication interference, particularly in overloaded scenarios where spatial resources are limited. This capability enhances the sensing-versus-communication trade-off, making NOMA-empowered ISAC designs more robust and efficient than conventional methods [3].

In uplink ISAC, NOMA facilitates the separation of communication signals and sensing echoes at the base station, ensuring reliable performance even in resource-constrained conditions. Through adaptive SIC decoding, uplink NOMA achieves higher throughput and sensing accuracy, surpassing orthogonal schemes. Additionally, NOMA supports dynamic resource allocation strategies, adapting to varying demands for sensing and communication. Studies show that NOMA-assisted ISAC systems deliver superior performance in high-mobility and dense network scenarios, positioning NOMA as a cornerstone for future ISAC technologies [4, 5].

Orthogonal Delay-Doppler Division Multiplexing (ODDM) is an innovative multicarrier modulation technique designed for high-mobility and doubly-selective wireless environments, leveraging the delay-Doppler (DD) domain for enhanced performance. Unlike traditional orthogonal frequency-division multiplexing (OFDM) or orthogonal time-frequency space (OTFS) modulation, ODDM employs orthogonal pulses explicitly aligned with the fine resolutions of the DD plane, enabling pre-

979-8-3315-2096-0/25/$31.00 ©2025 IEEE

cise coupling between transmitted signals and DD-domain channel characteristics [6, 7]. This coupling ensures minimal inter-symbol and inter-carrier interference, even under significant Doppler shifts, making ODDM particularly effective in high-speed scenarios such as vehicular networks and satellite communications [8].

In the context of ISAC, ODDM holds significant promise. Its orthogonal pulses in the DD domain allow simultaneous optimization of sensing and communication functionalities. For example, ODDM-based ISAC systems can effectively utilize the sparsity of DD channels for accurate sensing, while maintaining high data throughput for communication tasks. Studies have shown that ODDM outperforms OTFS in terms of bit error rate (BER) and out-of-band emission, demonstrating superior robustness in environments with high mobility and severe channel variations [9]. Additionally, ODDM's precise channel input-output relation supports efficient channel estimation and low-complexity symbol detection, further enhancing its utility in ISAC applications. By integrating sensing and communication in a unified framework, ODDM is poised to play a pivotal role in the development of next-generation wireless networks [10].

Integrating NOMA with ODDM in ISAC [11] systems enables efficient power allocation [12, 13], beamforming [14], and user grouping to maximize performance in high-mobility scenarios. NOMA's power allocation dynamically distributes resources across users based on channel conditions and communication-sensing priorities, while ODDM's precise delay-Doppler domain representation ensures minimal interference. Beamforming further enhances this synergy by directing power to desired users and sensing targets, leveraging ODDM's robust channel sparsity for improved accuracy. User grouping in NOMA, guided by channel correlations, pairs users with complementary resource demands, which ODDM supports through its orthogonal pulse design to maintain signal separation. Together, these techniques provide a robust framework for efficient resource utilization and superior communication-sensing integration.

The contributions of this paper are summarized below:

- We propose a NOMA-assisted ISAC-ODDM network architecture, where the ODDM modulation is formulated in the delay-Doppler domain.
- To improve system performances, we maximize the weighted sum of communication sum-rate and sensing performance metric by jointly optimizing power allocation, beamforming, and user grouping, which, however, are coupled. An efficient joint algorithm is then proposed, which decomposes the formulated problem into three subproblems and solves them in an iterative manner.
- Simulation results demonstrate that the considered NOMA-assisted ISAC-ODDM network can improve sum-rate and sensing accuracy compared to its couterpart using Orthogonal Multiple Access (OMA).

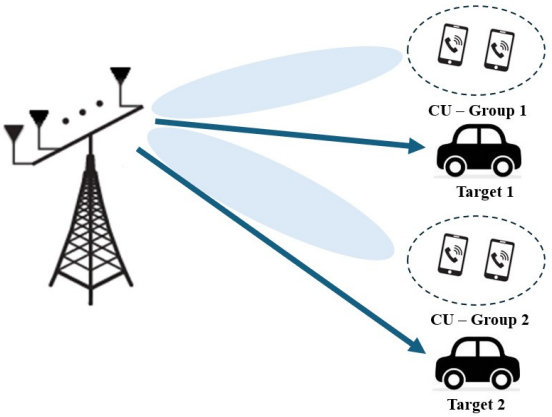

Fig. 1: ODDM ISAC Model.

II. Sytem Model

The ISAC-ODDM network enhanced with NOMA, as depicted in Fig. 1 that supports G clusters with P_g users in the g^{th} cluster, where $g \in \{1, 2, \ldots, G\}$. The base station (BS) is equipped with two planar antenna arrays: one for transmitting ODDM-based ISAC signals to all clusters and another for receiving echo signals from the sensing targets. The proposed system capitalizes on ODDM's robustness in delay-Doppler domain representation and NOMA's power domain multiplexing to enable efficient resource utilization while addressing multiple users.

A. ISAC Tx Signal Model

Consider the transmitted data symbols within one ODDM frame by the p^{th} user in the g^{th} cluster, represented as $U_{p,g}$. The ODDM frame consists of $M \times N$ data symbols, where M represents the number of time slots, and N indicates the number of subcarriers. The data symbol at the $(m, n)^{th}$ position in the DD domain for $U_{p,g}$ is denoted by $S_{p,g}(n, m)$. Following ODDM modulation, the modulated signal can be expressed as:

$$s_{p,g}(t) = \sum_{n=0}^{N-1} \sum_{m=0}^{M-1} S_{p,g}(n,m) u\left(t - m\frac{T}{M}\right) e^{j2\pi \frac{n}{NT}(t - m\frac{T}{M})}. \tag{1}$$

The signals of all users in the g-th cluster are superimposed via NOMA, i.e.,

$$s_g(t) = \sum_{p=1}^{P_g} \sqrt{\alpha_{p,g}} s_{p,g}(t). \tag{2}$$

where $\sqrt{\alpha_{p,g}}$ represnts the transmit power allocated to the p^{th} user $U_{p,g}$ in the g^{th} cluster. Stack the signals for G clusters as a vector $\vec{\mathbf{s}}(t) = [s_1(t), s_2(t), \ldots, s_G(t)]^T$. The aggregate transmitted signal after beamforming can be expressed as: $\vec{\mathbf{x}}(t) = \mathbf{A}\vec{\mathbf{s}}(t)$ where $\mathbf{A}$ is beamforming martix and $\mathbf{A} \in \mathbf{C}^{G\times G}$. Here we assume that the number of BS antennas are equal to the number of clusters G [7].

B. Rx Signal Model at the User in the Cluster

The received signal at user $U_{p,g}$, can be expressed as

$$\vec{\mathbf{y}}_{p,g}(t) = h_{p,g}\vec{\mathbf{c}}(\theta_{p,g})\,\vec{\mathbf{b}}^H(\theta_{p,g})\,\vec{\mathbf{x}}(t-\tau_{p,g})\,e^{j2\pi\nu_{p,g}t}, \tag{3}$$

where $\vec{\mathbf{c}}(\theta_{p,g})$ is the receiver beamsteering vector at $U_{p,g}$, $\vec{\mathbf{b}}^H(\theta_{p,g})$ is the transmitter beamsteering vector at BS, $\tau_{p,g}$ is the delay and $\nu_{p,g}$ is the doppler frequency shift. Rewriting $\mathbf{A}\vec{\mathbf{s}}(t)$ as $\sum_{g=1}^{G}\vec{\mathbf{a}}_g s_g(t)$ where $\vec{\mathbf{a}}_g$ is the g-th column of $\mathbf{A}$, and then the received signal in (3) can be rewritten as

$$\begin{aligned}\vec{\mathbf{y}}_{p,g}(t) &= h_{p,g}\vec{\mathbf{c}}(\theta_{p,g})\,\vec{\mathbf{b}}^H(\theta_{p,g})\,\vec{\mathbf{a}}_g s_g(t-\tau_{p,g})\,e^{j2\pi\nu_{p,g}t}\\ &+ \sum_{g'=g} h_{p,g}\vec{\mathbf{c}}(\theta_{p,g})\,\vec{\mathbf{b}}^H(\theta_{p,g})\,\vec{\mathbf{a}}_{g'} s_{g'}(t-\tau_{p,g})\,e^{j2\pi\nu_{p,g}t}\\ &+ \vec{\mathbf{n}}_{p,g}(t).\end{aligned} \tag{4}$$

Here the second term in the equation represents inter cluster interference and the third term represents noise. To mitigate inter-user interference $U_{p,g}$ user normalized equalizer

$$\vec{\mathbf{U}}_{p,g} = \frac{\vec{\mathbf{P}}_{p,g}}{|\vec{\mathbf{P}}_{p,g}|}, \tag{5}$$

where $\vec{\mathbf{P}}_{p,g}$ is the g-th cloumn of $\mathbf{P}_{p,g}\left(\mathbf{P}_{p,g}^H\mathbf{P}_{p,g}\right)^{-1}$, $\mathbf{P}_{p,g} = \mathbf{H}_{p,g}\mathbf{A}$, and $\mathbf{H}_{p,g} = h_{p,g}\vec{\mathbf{c}}(\theta_{p,g})\,\vec{\mathbf{b}}^H(\theta_{p,g}) \in C$. After equalization, the received signal is,

$$\begin{aligned}\hat{\mathbf{y}}_{p,g}(t) &= \vec{\mathbf{U}}_{p,g}^H h_{p,g}\vec{\mathbf{a}}_g s_g(t-\tau_{p,g})\,e^{j2\pi\nu_{p,g}t}\\ &+ \vec{\mathbf{U}}_{p,g}^H\vec{\mathbf{n}}_{p,g}(t).\end{aligned} \tag{6}$$

Perform ODDM demodulation to $\hat{\mathbf{y}}_{p,g}(t)$, we can derive

$$\begin{aligned}\vec{\mathbf{Y}}_{p,g}[m,n] &= \vec{\mathbf{U}}_{p,g}^H H_{p,g}\vec{\mathbf{a}}_g\hat{s}_g(\hat{m},\hat{n})\,e^{j2\pi\frac{k_p(m-l_p)}{MN}}\\ &+ \mathbf{n}_s(m,n).\end{aligned} \tag{7}$$

Here,

$$\hat{s}_g(\hat{m},\hat{n}) = \begin{cases}\sum_{p=1}^{P_g}\sqrt{\alpha_{p,g}}s_{p,g}(m,n), & \hat{m}\geqslant 0.\\ \sum_{p=1}^{P_g}\sqrt{\alpha_{p,g}}s_{p,g}(m+\hat{m},\hat{n}), & \hat{m}\leqslant 0.\end{cases} \tag{8}$$

where $\hat{m} = m - l_p$, $\hat{n} = [n-k_p] \bmod N$, $l_p = \tau_p\frac{M}{T}$ and $k_p = \nu_p NT$.

Assume effective channel $\mathbf{U}_{p,g}^H H_{p,g}\vec{\mathbf{a}}_g$ for $U_{p,g}$ satisfies

$$\mathbf{U}_{1,g}^H H_{1,g}\vec{\mathbf{a}}_g \leqslant \mathbf{U}_{2,g}^H H_{2,g}\vec{\mathbf{a}}_g \ldots \leqslant \mathbf{U}_{p_g,g}^H H_{p_g,g}\vec{\mathbf{a}}_g. \tag{9}$$

Therefore, the rate for $U_{p,g}$ is

$$R_p = \min\{R_{p\to p}, \ldots, R_{p\to p_g}\}, \tag{10}$$

where

$$R_{p\to j} = \log_2\left(1 + \frac{|\sqrt{\alpha_{p,g}}\vec{\mathbf{U}}_{j,g}^H H_{j,g}\vec{\mathbf{a}}_g|^2}{\sum_{i>p}|\sqrt{\alpha_{i,g}}\vec{\mathbf{U}}_{j,g}^H H_{j,g}\vec{\mathbf{a}}_g|^2 + \sigma^2}\right). \tag{11}$$

$$R_P = \log_2\left(1 + \frac{|\sqrt{\alpha_{p,g}}\vec{\mathbf{U}}_{j,g}^H H_{j,g}\vec{\mathbf{a}}_g|^2}{\sigma^2}\right). \tag{12}$$

C. Sensing performance

The covariance of the transmitter signal of the ISAC transceiver is

$$R_w = \mathbf{E}\left(\vec{\mathbf{x}}(t)\vec{\mathbf{x}}^H(t)\right). \tag{13}$$

$$R_w = \sum_g\left(M\sum_p\alpha_{p,g}\right)\vec{\mathbf{a}}_g\vec{\mathbf{a}}_g^H. \tag{14}$$

where $M = \mathbf{E}\left(|\mathbf{s}_{pg}(t)|\right)^2$

Therefore, the cross correlation between two target directions θ_k, θ_p is

$$\mathbf{C}(\theta_k,\theta_p) = |\vec{\mathbf{b}}^H(\theta_k)\,R_w\vec{\mathbf{b}}(\theta_p)|, \tag{15}$$

where $\vec{\mathbf{b}}(\theta_p)$ is steering vector at the BS. Therefore, mean square cross correlation is

$$\bar{\mathbf{C}} = \frac{2}{S^2-S}\sum_{k=1}^{S-1}\sum_{p=k+1}^{S}\mathbf{C}^2(\theta_k,\theta_p), \tag{16}$$

where S represents number of sensing targets. Besides the signal power in the target direction θ_S is

$$\mathbf{P}(\theta_S) = \vec{\mathbf{b}}^H(\theta_S)\,R_w\vec{\mathbf{b}}(\theta_S). \tag{17}$$

III. Problem Formulation

The joint optimization problem for user grouping, beamforming, and power allocation is formulated as:

$$\max_{\substack{\{\alpha_{p,g}\},\{C_g\}\\ \{\vec{\mathbf{a}}_g\}}} \rho_C\sum_p R_p + \rho_S\sum_S P(\theta_S) \tag{18}$$

$$\text{subject to} \quad \bar{\mathbf{C}} \leqslant \epsilon, \tag{19}$$

$$R_p \geqslant R_{min}, \tag{20}$$

$$Tr(R_w) \leqslant P_{\vec{\mathbf{a}}_g}, \tag{21}$$

$$\mathbf{C}_g \cap \mathbf{C}_{g'} = \varnothing, \mathbf{C}_g \neq \varnothing. \tag{22}$$

where $\alpha_{p,g}$ is power allocation to $U_{p,g}$, C_g is the set of user index belonging to the g-th cluster and $\vec{\mathbf{a}}_g$ is the g-th cloumn of beamforimg matrix $\mathbf{A}$ are the Optimization variable. ρ_C, ρ_S is weight for communication and sensing to regularize the tradeoff, R_p is the data rate for $U_{p,g}$ and $P(\theta_S)$ is the signal power in sensing target direction θ_S. Tr(•) denotes the trace operation. Here, constraint (19) guarantees sensing performance and constraint (20) ensures the

minimum data rate of each user. Constraint (21) indicates maximum transmit power. Constraint (22) shows that each user belongs to one cluster, and each cluster contains at least one user.

A. Problem Decomposition

It is challenging to solve the optimization problem in (55) since the power allocation, user grouping, and beamforming are coupled. To address the complexities of optimizing the NOMA-assisted ISAC-ODDM framework, the joint problem of user grouping, power allocation, and beamforming is decomposed into three interconnected subproblems, i.e., power allocation subproblem, beamforming subproblem, and user grouping subproblem., where the three subproblems are solved in an iterative manner so as to improve both communication and sensing performances. This decomposition ensures computational tractability while achieving a balanced trade-off between communication throughput and sensing accuracy. Specifically, given the beamforming $\vec{\mathbf{a}}_g$ and user grouping $\{C_g\}$, the power allocation subproblem, which determines the optimal power to assign to each user $\alpha_{p,g}$ within the cluster, balancing the requirements for communication and sensing, can be given by

$$\max_{\{\alpha_{p,g}\}} \rho_C \sum_{p\in C_g} R_p + \rho_S \sum_S P(\theta_S) \tag{23}$$

$$\text{subject to} \quad R_p \geqslant R_{min}, \quad \forall p \in C_g, \tag{24}$$

$$\sum_{p=1} \alpha_{p,g} = 1, \quad \forall g, \tag{25}$$

$$\alpha_{p,g} \in (0,1), \ \forall p, g. \tag{26}$$

Given the power allocation $\alpha_{p,g}$ and user grouping C_g, the beamforming subproblem can be given by

$$\max_{\vec{\mathbf{a}}_g} \rho_C \sum_{p\in C_g} R_p + \rho_S \sum_S P(\theta_S) \tag{27}$$

$$\text{subject to} \quad R_p \geqslant r_p, \ \forall g, p, \tag{28}$$

$$\sum_{g=1}^{G} \|\mathbf{w}_g\|_2^2 \leqslant P_t. \tag{29}$$

Then, by fixing the power allocation and beamforming, the user grouping subproblem can be given by

$$\max_{\{C_g\}} \rho_C \sum_p R_p + \rho_S \sum_S P(\theta_S) \tag{30}$$

$$\text{subject to} \quad \bar{\mathbf{C}} \leqslant \epsilon, \tag{31}$$

$$R_p \geqslant R_{min}, \tag{32}$$

$$Tr(R_w) \leqslant P_{\mathbf{a}_g}, \tag{33}$$

$$\mathbf{C}_g \cap \mathbf{C}_{g'} = \varnothing, \mathbf{C}_g \neq \varnothing. \tag{34}$$

Algorithm 1 Power allocation for NOMA-ISAC

1: **Input:** ρ_C, ρ_S, $R_{\min}$, σ^2, $\alpha_{p,g}$, η, δ, and ϵ_1, ϵ_2
2: Update $\alpha_{p,g}$ using the iterative closed-form expressions in Equ.(35-37):
3: Formulate the penalty-based optimization problem:

$$\max_{\alpha_{p,g}} \rho_C \sum_{p\in C_g} R_p + \rho_S \sum_S P(\theta_S) - \frac{1}{\eta} \sum_{p\in C_g} (\|\alpha_{p,g}\|_* - \|\alpha_{p,g}\|_2)$$

4: Update $\alpha_{p,g}^{(n+1)}$
5: Increment n: $n \leftarrow n+1$
6: Update $\alpha_{p,g} \leftarrow \alpha_{p,g}^{(n)}$
7: Reduce penalty factor: $\eta \leftarrow \delta \cdot \eta$
8: **Return:** Optimized power allocation $\alpha_{p,g}$ for all users

IV. Joint power allocation, beamforming, and user grouping optimization algorithm design

A. Power Allocation

To maximize the sum rate of all users, the power allocation problem becomes maximizing the sum rate in each cluster, respectively. For all $p_0 \in \{1, \ldots, P_g - 1\}$, if all $\alpha_{g,p}, p \in \{1, \ldots, p_0-1, p_0+2, \ldots, P_g\}$ are fixed, R_p is non-increasing with α_{g,p_0} increasing. Accordingly, the closed form expression for the optimal power allocation in iteration i can be obtained as [15]

$$\alpha_{1,g}^{(i)} = \frac{\gamma_{1,g}^{th}}{1+\gamma_{1,g}^{th}} \left(1 + \frac{\sigma_0^2}{|\vec{\mathbf{U}}_{1,g}^H H_{1,g} \vec{\mathbf{a}}_g|_2^2}\right), \tag{35}$$

$$\vdots$$

$$\alpha_{P_g-1,g}^{(i)} = \frac{\gamma_{P_g-1,g}^{th}}{1+\gamma_{P_g-1,g}^{th}} \left(1 - \sum_{j=1}^{P_g-2} \alpha_{j,g} + \frac{\sigma_0^2}{|\vec{\mathbf{U}}_{P_g-1,g}^H H_{P_g-1,g} \vec{\mathbf{a}}_g|_2^2}\right), \tag{36}$$

$$\alpha_{P_g,g}^{(i)} = 1 - \sum_{p=1}^{P_g-1} \alpha_{p,g}, \tag{37}$$

where $\gamma_{p,g} = 2^{R_p^{th}} - 1$ denotes the signal-to-interference-and-noise ratio (SINR) threshold for $U_{p,g}$. Algorithm 1 outlines the iterative process, incorporating penalty terms to regularize the optimization and enhance convergence.

B. Beamforming

Note that the beamforming vector can affect the system performance by influencing the covairance matrix $\mathbf{R}_w$. Therefore, by introducing an additional vector $\mathbf{w}_g$ which satisfies $\mathbf{R}_w = \mathbf{w}_g \mathbf{w}_g^H$, the beamforming problem can be rewritten as

$$\max_{r_p,\mathbf{W}_p} \; f(\rho_c,\rho_s,r_p,\mathbf{W}_p)=\rho_C\sum_p R_p+\rho_S\sum_S P(\theta_S)$$

$$R_P \geqslant r_P \tag{38}$$

$$r_p \geqslant R_{\min,p}, \quad \forall p\in\mathcal{P} \tag{39}$$

$$\mathbf{A}_p \succeq 0, \mathbf{A}_p=\mathbf{A}_p^H, \quad \forall p\in\mathcal{P} \tag{40}$$

where $\mathbf{H}_p = \mathbf{h}_p\mathbf{h}_p^H$, $\mathbf{A}_p = \mathbf{a}_p\mathbf{a}_p^H$, $\mathbf{h}_p = \sqrt{\alpha_{p,g}}\vec{\mathbf{U}}_{j,g}^H H_{j,g}\vec{\mathbf{a}}_g$, and $\mathbf{a}_p = \left(M\sum_p \alpha_{p,g}\right)\vec{\mathbf{a}}_g$. By use the successive convex approximation (SCA) method and the non-convex constraint can be rewritten as

$$R_{p\to j} = \log_2\left(\sigma^2+\sum_{i\in p_g, i\geqslant p}\mathrm{Tr}\left(\mathbf{H}_j\mathbf{W}_i\right)\right) \underbrace{-\log_2\left(\sigma^2+\sum_{i\in p_g, i>p}\mathrm{Tr}\left(\mathbf{H}_j\mathbf{W}_i\right)\right)}_{F_{j,p}} \geqslant r_p. \tag{41}$$

By using the first-order Taylor expansion,

$$F_{j,p}\geqslant \widehat{F}_{j,p}\triangleq -\log_2\left(\sigma^2+\sum_{i\in p_g,i>p}\mathrm{Tr}\left(\mathbf{H}_j\mathbf{W}_i^n\right)\right) - \frac{\sum_{i\in p_g,i>p}\mathrm{Tr}\left(\mathbf{H}_j\left(\mathbf{W}_i-\mathbf{W}_i^n\right)\right)}{\left(\sigma^2+\sum_{i\in p_g,i>p}\mathrm{Tr}\left(\mathbf{H}_j\mathbf{W}_i^n\right)\right)\ln 2}. \tag{42}$$

Define,

$$\widehat{R}_{p\to j}\triangleq \log_2\left(\sigma^2+\sum_{i\in\mathcal{P},i\geqslant p}\mathrm{Tr}\left(\mathbf{H}_j\mathbf{W}_i\right)\right)+\widehat{F}_{j,p} \tag{43}$$

We introduce a penalty term to the objective function as in [14]

$$\max_{r_p,\mathbf{W}_p} \; f(\rho_c,\rho_s,r_p,\mathbf{W}_p)-\frac{1}{\eta}\sum_{p\in\mathcal{P}}\left(\|\mathbf{W}_p\|_*+\widehat{\mathbf{W}}_p^n\right) \tag{44}$$

$$|P(\theta_k)-P(\theta_p)|\leqslant P_{\text{diff}}, \quad \forall k\neq p\in\mathcal{M} \tag{45}$$

$$\mathrm{diag}\left(\sum_{i\in\mathcal{P}}\mathbf{w}_i\mathbf{w}_i^H\right)=\frac{P_t\mathbf{1}^{N\times 1}}{N} \tag{46}$$

$$\bar{C}\leqslant\epsilon \tag{47}$$

$$r_p\geqslant R_{\min,p}, \quad \forall p\in\mathcal{P} \tag{48}$$

$$\mathbf{W}_p\succeq 0, \mathbf{W}_p=\mathbf{W}_p^H, \quad \forall p\in\mathcal{P} \tag{49}$$

$$\widehat{R}_{p\to j}\geqslant r_p, \quad j\geqslant p,\ \forall p\in\mathcal{P},\ p\neq\mathcal{P}, \tag{50}$$

$$R_P\geqslant r_p \tag{51}$$

The choice of the parameter η plays a critical role in the optimization process for the NOMA-assisted ISAC-ODDM framework. Specifically, setting $\frac{1}{\eta}\to\infty$ ensures that the rank of the beamforming matrix $\mathbf{W}_g$ becomes one. However, in this scenario, the objective function is heavily influenced by the penalty term, leading to suboptimal solutions for throughput maximization and effective sensing power. To mitigate this, the algorithm initializes η with a large value, providing a solid starting point for optimizing throughput and sensing power. The overall algorithm, summarized in Algorithm 2.

Algorithm 2 Beamforming for NOMA-ISAC

1: **Input:** ρ_C, ρ_S, $R_{\min}$, σ^2, $\alpha_{p,g}$, η, δ, ϵ_1, ϵ_2
2: Initialize the feasible beamforming matrices $W_p^{(0)}$, $\forall p\in\mathcal{P}$.
3: Set iteration counters $n=0$.
4: **repeat**
5: **repeat**
6: Update $W_p^{(n+1)}$ by solving the optimization problem:
$$\max_{A_p} f(\rho_C,\rho_S,R_p,A_p)-\frac{1}{\eta}\sum_{p\in\mathcal{P}}\left(\|\mathbf{W}_p\|_*+\widehat{\mathbf{W}}_p^n\right)$$
7: Constraints:
1) $R_p\geqslant R_{\min,p},\ \forall p$
2) $\|W_p\|\leqslant P_{\text{ag}},\ \forall p$
3) $\tilde{C}\leqslant\epsilon$
4) $R_{p\to j}\geqslant R_p,\ j\geqslant p,\ \forall p\neq P$
8: Increment inner iteration counter: $n\leftarrow n+1$.
9: **until** Fractional reduction of the objective function value falls below ϵ_1.
10: Update initial beamforming matrices: $W_p^{(0)}\leftarrow W_p^{(n)}$, $\forall p\in\mathcal{P}$.
11: Update penalty factor: $\eta\leftarrow\delta\cdot\eta$.
12: **until** $\sum_{p\in\mathcal{P}}(\|W_p^{(n)}\|_*-\|W_p^{(n)}\|_2)\leqslant\epsilon_2$.
13: **Output:** Optimized beamforming matrices $W_p^\star$ achieving the trade-off between communication throughput and sensing performance.

C. User Grouping

Cluster users to maximize overall system performance:

$$\max_{\{C_g\}}\rho_C\sum_{p\in C_g}R_p+\rho_S\sum_S P(\theta_S) \tag{52}$$

$$\text{subject to} \quad \mathbf{C}_g\cap\mathbf{C}_{g'}=\varnothing, \mathbf{C}_g\neq\varnothing, \quad \forall g, \tag{53}$$

$$R_p\geqslant R_{min}, \quad \forall p\in C_g, \tag{54}$$

$$r_{p,q}=\beta. \tag{55}$$

where $r_{p,q}=\frac{||h_p^H h_q||}{||hp||||hq||}$ represent the channel correlation and β is the minimum correlation coefficient for which two users' Rayleigh fading channel gains are considered to be correlated. This formulation ensures an efficient balance between communication and sensing objectives, leveraging insights from advanced NOMA and ODDM studies. Algorithm 3 provides a systematic approach for user grouping,

Algorithm 3 NOMA User Grouping

Initialize: Total clusters G, user groups $C_g = \varnothing$ for $g = 1, 2, \ldots, G$.
Set weights ρ_C and ρ_S for communication and sensing priorities.
Initialize minimum correlation coefficient threshold β.
Calculate:
for all user pairs (p, q) **do**
    Compute channel correlation $r_{p,q} = \frac{|\mathbf{h}_p^H \mathbf{h}_q|}{\|\mathbf{h}_p\| \|\mathbf{h}_q\|}$.
    Calculate contributions to communication R_p.
end for
Assign Cluster Heads:
Sort users in descending order of channel gain.
Select the top G users as initial cluster heads H_g for $g = 1, 2, \ldots, G$.
Iterative User Grouping: For each user p not yet assigned to a cluster g evaluate $r_{p,g}$ based on channel correlation with cluster head.
if $r_{p,g} \geqslant \beta$ **then**
    Assign p to C_g.
    Update C_g and recompute cluster sum rate $\sum_{p \in C_g} R_p$.
end if
Iterate over clusters to reassign users.
Ensure all clusters satisfy:
    $R_p \geqslant R_{\min}$.
Output:
Return optimized user groupings C_g.

iteratively refining assignments to optimize communication and sensing metrics.

V. Simulation Results

The simulation setup considers a multi-user communication system utilizing ODDM modulation for high-mobility users and NOMA for low-mobility users. The ODDM grid is defined with $M = 512$ subcarriers and $N = 64$ time slots, with a subcarrier spacing of $\Delta f = 15$ kHz and a symbol duration $T = \frac{1}{\Delta f}$. The channel model is doubly selective, featuring 3-6 propagation paths characterized by delays uniformly distributed within $[0, T]$, Doppler shifts within $[-v_{max}, v_{max}]$, with $v_{max} = 500$km/h. carrier frequency is $f_c = 5$ GHz and path gains following a complex Gaussian distribution $\mathcal{CN}(0, \frac{1}{P})$, where P is the number of paths. Transmit power is varied between 0 dBm and 30 dBm, and noise levels are modeled as AWGN. Key performance metrics include SINR, achievable sum-rate, and signal power evaluated over multiple channel realizations.

Fig. 2 illustrates the sum-rate performance of NOMA and OMA systems in the context of ODDM modulation under varying transmit power and user mobility conditions. The integration of NOMA with ODDM modulation demonstrates superior performance across all scenarios, leveraging ODDM's capability to effectively handle doubly selective channels and mitigate the impact of Doppler effects in high-mobility environments. The figure shows that NOMA achieves significantly higher sum rates compared to OMA, particularly in high-speed scenarios such as 500 km/h, where the delay-Doppler domain representation of ODDM ensures resilience against channel variations. Additionally, the performance gap between NOMA and OMA increases with higher transmit power, highlighting the robustness of the NOMA-assisted ODDM system. These results confirm the effectiveness of the NOMA-ODDM framework in addressing the challenges of high-mobility and high-speed communication environments, making it a promising solution for next-generation wireless networks.

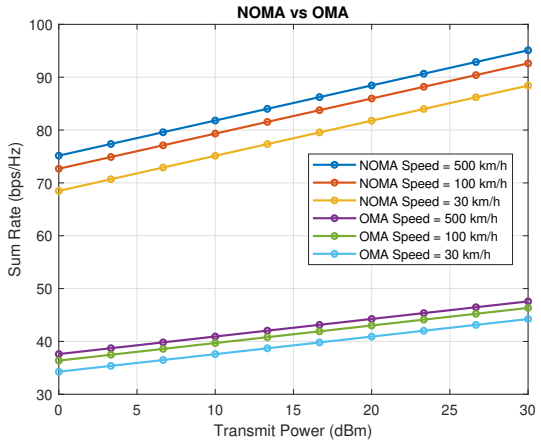

Fig. 2: Sum-rate versus transmit power.

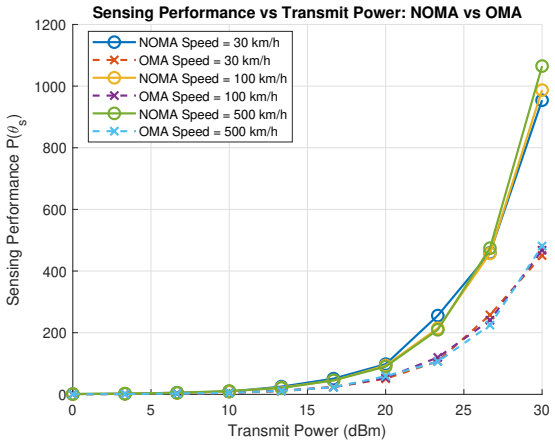

Fig. 3: Sensing performance versus transmit power.

The relationship between sensing performance $P(\theta_S)$ and transmit power is presented in Fig. 3, highlighting comparisons between NOMA and OMA systems across user mobility speeds of 30 km/h, 100 km/h, and 500 km/h. The sensing performance improves with increasing transmit power, reflecting enhanced signal strength and detection capabilities.

NOMA consistently outperforms OMA in all scenarios due to its efficient resource allocation and robustness in integrating communication and sensing functionalities.

At lower transmit power levels (below 20 dBm), the difference between NOMA and OMA systems is less pronounced. However, as the transmit power increases, NOMA demonstrates a significant performance advantage, particularly at high mobility speeds (e.g., 500 km/h). This indicates the ability of the NOMA-assisted framework to maintain reliable sensing accuracy in dynamic environments where Doppler shifts and channel variations are prominent. Furthermore, the ODDM modulation employed in both systems ensures resilience to high-mobility challenges, but the synergy between NOMA and ODDM in managing interference and optimizing resources amplifies the sensing capabilities of the NOMA system.

VI. Conclusion

This paper introduces the integration of NOMA and ODDM within an ISAC framework, optimizing resource utilization and enhancing performance in high-mobility scenarios. By leveraging ODDM's robustness in the delay-Doppler domain and NOMA's ability to serve multiple users simultaneously, the proposed framework achieves improved communication throughput and sensing accuracy. Through the design of power allocation, beamforming, and user grouping, the system effectively addresses the challenges of dynamic and high-mobility environments. The results show that at a transmit power of 30 dBm and a mobility of 500 km/h, the NOMA-assisted ODDM system achieves a sum-rate of nearly 100 bps/Hz, significantly outperforming the OMA system's 70 bps/Hz, while also enhancing sensing performance by over 22%. These findings demonstrate the robustness and efficiency of the NOMA-assisted ODDM framework, thereby establishing it as a promising solution for next-generation ISAC networks and a foundation for future research into advanced ISAC designs.

References

[1] H. Zhang, H. Zhang, B. Di, M. Di Renzo, Z. Han, H. V. Poor, and L. Song, "Holographic Integrated Sensing and Communication," *IEEE J. Sel. Areas Commun.*, vol. 40, no. 7, pp. 2114–2130, Jul. 2022.

[2] K. Meng, Q. Wu, W. Chen, and D. Li., "Sensing-Assisted Communication in Vehicular Networks with Intelligent Surface,"*IEEE Veh. Trans. Veh. Technol.*, vol. 73, no. 1, pp. 876-893, Jan. 2024.

[3] X. Mu, Z. Wang, and Y. Liu., "NOMA for Integrating Sensing and Communications Toward 6G: A Multiple Access Perspective," *IEEE Wireless Commun.*, vol. 31, no. 3, pp. 316–323, Jan. 2024.

[4] L. Sun, Z. Zhao, S. Wang, Z. Ding, and M. Peng, "On the Study of Non-Orthogonal Multiple Access (NOMA)-Assisted Integrated Sensing and Communication (ISAC)," *IEEE Trans. Commun.*, vol. 72, no. 11, pp. 7278–7293, May 2024.

[5] Z. Kang, H. Zhao, and H. Wang, "An Efficient TwoDimension OTFS-NOMA Scheme Based on Heterogenous Mobility Users Grouping," in *IEEE 21st International Conference on Communication Technology (IEEE ICCT)*, Tianjin, China, Nov. 2021

[6] H. Lin and J. Yuan, "Multicarrier Modulation on Delay-Doppler Plane: Achieving Orthogonality with Fine Resolutions," in *IEEE International Conference on Communications (IEEE ICC)*, Seoul, South Korea, May 2022.

[7] H. Lin and J. Yuan, "Orthogonal Delay-Doppler Division Multiplexing Modulation," *IEEE Trans. Wireless Commun.*, vol. 21, no. 12, pp. 11024-11037, Jul. 2022.

[8] K. Huang, M. Qiu, J. Tong, J. Yuan, and H. Lin, "Performance of ODDM with Imperfect Channel Estimation," in *IEEE 24th International Workshop on Signal Processing Advances in Wireless Communications (IEEE SPAWC)*, Shanghai, China, Nov. 2023.

[9] D. Wang, C. Huang, L. Liu, X. Chen, W. Wang, Z. Zhang, C. Yuen, and M. Debbah., "Exploring Channel Estimation and Signal Detection for ODDM-Based ISAC Systems," *IEEE Wireless Commun. Lett.*, vol. 13, no. 8, pp. 2270–2274, Jun. 2024.

[10] J. Tong, J. Yuan, H. Lin, and J. Xi, "Orthogonal Delay-Doppler Division Multiplexing (ODDM) Over General Physical Channels,"*IEEE Trans. Commun.*, to be published.

[11] L. Xiang, K. Xu, J. Hu, C. Masouros, and K. Yang, "Robust NOMA-Assisted OTFS-ISAC Network Design With 3-D Motion Prediction Topology,"*IEEE IoT J.*, vol. 11, no. 9, pp. 15909–15918, Jan. 2024.

[12] J. Li, T. Gao, B. He, W. Zheng, and F. Lin, "Power Allocation and User Grouping for NOMA Downlink Systems," *Appl. Sci.*, vol. 13, no. 4, pp. 1-6, Feb. 2023.

[13] J. Zhu, Q. Li, Z. Liu, H. Chen, and H. V. Poor, "Enhanced User Grouping and Power Allocation for Hybrid mmWave MIMO-NOMA Systems," *IEEE Trans. Wireless Commun.*, vol. 21, no. 3, pp. 2034– 2050, Sep. 2022.

[14] Z. Wang, Y. Liu, X. Mu, Z. Ding, and O. A. Dobre, "NOMA Empowered Integrated Sensing and Communication,"*IEEE Commun. Lett.*, vol. 26, no. 3, pp. 677–681, Jan. 2022.

[15] W. Lyu, Y. Xiu, X. Li, S. Yang, P. L. Yeoh, Y. Li, and Z. Zhang, "Hybrid NOMA-Assisted Integrated Sensing and Communication via RIS," *IEEE Trans. Veh. Technol.*, vol. 73, no. 5, pp. 7368–7373, Dec. 2023.